Enhancing the performance of CO2-based refrigeration cycles using the Ranque-Hilsch vortex tube process

Wojciech Kostowski[a], Michał Majchrzyk[b], Barbara Mendecka[c], Marcel Barzantny[d], Daniele Chiappini[e], Bartosz Łomiński[f] and Paweł Bargiel[g]

[a] *Silesian University of Technology, Gliwice, Poland, wojciech.kostowski@polsl.pl CA*
[b] *Silesian University of Technology, Gliwice, Poland, michal.majchrzyk@polsl.pl*
[c] *Niccolo Cusano University, Rome, Italy, barbara.mendecka@unicusano.it*
[d] *Silesian University of Technology, Gliwice, Poland, marcel.barzantny@polsl.pl*
[e] *Niccolo Cusano University, Rome, Italy, daniele.chiappini@unicusano.it*
[f] *Silesian University of Technology, Gliwice, Poland, bl308683@student.polsl.pl*
[g] *Silesian University of Technology, Gliwice, Poland, pawel.t.bargiel@gmail.com*

Abstract:
The paper presents a thermodynamic study on enhancing the performance of CO_2-based vapour compression refrigeration cycles by applying the Ranque-Hilsch vortex tube. Two possible configurations are analysed: the RHVT Maurer refrigeration cycle operating with a 3-flow vortex tube, and the RHVT Keller cycle, operating with gaseous phase only. For both configurations, a system flow diagram was set, and a thermodynamic model has been developed in the EES environment. The model comprises first- and second-law analysis to identify valid areas of operation. It has been shown that the coefficient of performance may exceed the reference value of a standard CO_2-based cycle, however, it is possible under a limited range of vortex tube parameters. In particular, the 3-flow vortex tube requires a substantial fraction of liquid to be collected and extracted to provide a positive overall thermodynamic effect. For the Keller model and the 2-flow vortex tube the possible area of operation is also constrained. It has been demonstrated that both configurations may be a promising alternative for industrial/large scale refrigeration in warm climates, however, the technology readiness level remains low, opening field for further research.

Keywords:
Vortex Tube, Ranque-Hilsch effect, Refrigeration, R744 refrigerant, transcritical CO_2 cycle

1. Introduction

In a standard refrigeration cycle, a throttle valve is used, which causes an increase in entropy and irreversible changes resulting from the pressure drop by throttling. The process itself is isenthalpic and the refrigerant transitions to a liquid state completing the Linde cycle. Thanks to the valve's simple design, it is a reliable solution but it fails to utilise the high-pressure potential for a possible increase in cycle performance. Therefore, it may be meaningful to replace the throttle valve with a Ranque'a-Hilsch vortex tube (RHVT), which expands and splits the high-pressure inlet flow into two streams with different temperature levels, commonly referred to as 'cold' and 'hot' [1, 2].
Initially, from the time of its invention in 1933, the RHVT was primarily used for for energy separation as a cooling device for various technological processes such as for laboratory equipment cooling [3] or controlling the temperature of CNC machines [4], and occasionally also as a device for separating mixtures e.g. in the sea water desalination process [5]. It was not until the end of the millennium, in 1997, that Keller and Göbel proposed using the RHVT as a replacement of the throttle valve to improve the coefficient of performance (COP) of the refrigeration cycle [6]. The implementation involved redirecting the gas fraction remaining after conventional throttling to the inlet of the RHVT valve. The hot outlet stream is then cooled in a desuperheater, recirculated to the cold stream and both

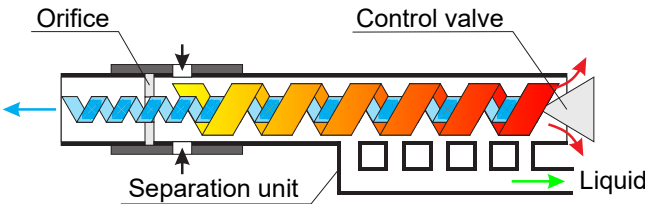

Figure 1: Technical solution for the phase change process

are fed into the compressor inlet at the same time. However, the original concept does not address liquefaction of the agent in the separation unit when fed with saturated medium. Maurer proposed a solution to this problem in his patent [7], combining a 3-way vortex tube (a vortex tube with an additional outlet for the condensing agent) with a new refrigeration system layout. Since then, a few system enhancements were proposed, the latest findings are described in detail in recent review papers [8, 9].

The concept of the 3-way vortex tube for phase change processes with an additional outlet in the separation unit, which is perforated in a form of slotted gaps, through which the condensate is drained has been known for a few decades. Lately, the slot geometry and its position was studied experimentally by Liang et al. [10]. Results showed a removal of up to 77% of humid air. The concept of a such vortex tube is shown in Fig. 1.

The proposed implementation of a RHVT into a refrigeration cycle can provide up to 37% COP improvement assuming an ideal expansion process for the t-CO_2 cycle compared to the isenthalpic expansion with evaporation at 5 °C and a gas cooler outlet temperature of 40 °C [11]. The proposed system was studied by Xie et al. achieving a COP improvement of 2.4-16.3% for a two-stage transcritical CO_2 cycle [12]. A similar investigation with identical conditions was conducted by Liu et al. [13]. In a case of this study, the COP of the heat pump cycle increased by 5.3-13.9%. However, both studies did not provide details on the flow and temperature distribution in the RHVT. Another numerical study of the t-CO_2 cycles was investigated by Khera et al. obtaining a similar COP improvement of 27% [14]. The Keller and Maurer models were also investigated and compared numerically by [15] et al. The authors reported a substantial increase of performance for the Maurer system at the level of 24% in comparison to the standard cycle with a throttle valve. The models were validated using publicly available experimental data. Luo et al. conducted research on optimizing the Maurer system using various RHVT values and serial and parallel configurations [16]. The numerical model showed COP enhancement of up to 27%; the authors stated, that the optimum configuration depends on the number of evaporators in the system and cold mass fraction working conditions. Chen et al. investigated the t-CO_2 cycle experimentally, but the obtained temperature differences were marginal due to the low inlet-outlet pressure differentials [17]. The authors reported that the cooling effect of the vortex tube depends on the phase state at the cold outlet and for a case of two-phase outlet, the performance is higher than for the isenthalpic and isentropic expansions. Different experimental t-CO_2 cycle investigation showed a similar temperature drop at 1.18 °C when the inlet pressure level was about 82 bar [18]. Both studies represents an enormous effect deterioration in comparison to the numerical models. A different application was investigated by Mendecka et al. [19]. The study was focused on the COP improvements for t-CO_2 cycle for electric vehicles. The observed improvement of COP was estimated at 5-17%.

The objective of the current work is to provide a deeper thermodynamic insight in the possiblity of achieving actual improvements with respect to the reference cycle with a throttle valve. This is done by a parametric assesment of the previously known Keller and Maurer configuration; additionally, each configuration and each set of parameters were subject to a 2nd law-based exergy test, to check if the given point of operation is possible to obtain in real conditions. Moreover, the paper also provides a preliminary numerical model to assess the operation of the vortex tube under 2-phase conditions.

2. Methods

The method of analysis comprises a definition of system superstructure, formulation of mass and energy balance equations and derivation of system performance indicators. For each of the two studied system configurations, the analytical chain has been described independently.

2.1. The Maurer model

2.1.1. Model structure

A superstructure of the Maurer model including the reference refrigeration cycle is shown in Fig. 2.

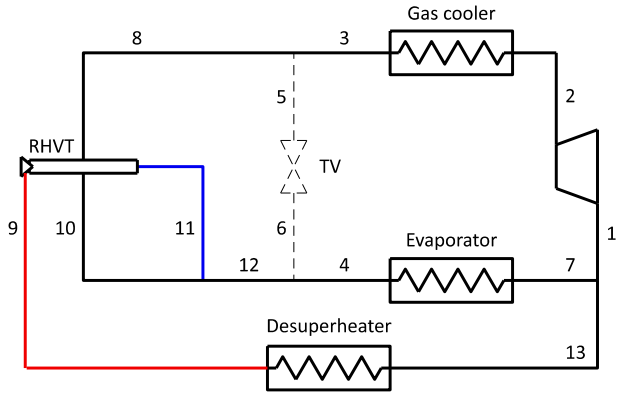

Figure 2: A superstructure of the Maurer model including the reference refrigeration cycle

The superstructure simultaneously includes the reference refrigartion cycle with a throttle valve and the extended version with a 3-fluid vortex tube. The operation of the cycles is defined as follows:

The reference refrigeration cycle, comprised of four elements: a compressor, a gas cooler, a throttle valve (TV) and an evaporator is represented by system points 1–4. For the reference case, the working agent 1 is compressed to state 2, cooled to state 3 and then it is directed to the throttle valve, while there is no flow through the RHVT section. Furthermore, the thermodynamic states $\Phi = (p, T, v)$ in some adjacent points are identical by definition. Accordingly:

$$\dot{m}_i = \dot{m}, \quad i \in \{1, 2, 3, 4, 5, 6, 7\} \tag{1}$$

$$\dot{m}_j = 0 \quad j \in \{8, 9, 10, 11, 12, 13\} \tag{2}$$

$$\Phi_5 = \Phi_3, \quad \Phi_6 = \Phi_4, \quad \Phi_1 = \Phi_7 \tag{3}$$

The RHVT Maurer refrigeration cycle, uses the compressed, cooled gas at point 3 as inlet (8) agent to a Ranque-Hilsch vortex tube. The RHVT has three outlets:

1. the hot, gaseous outlet 9 extracted through the RHVT regulating valve;
2. the liquid outlet 10, collecting droplets at the tube circumference;
3. the cold outlet, expected to carry dry, saturated gas.

The liquid and the cold outlet are joined downstream of the RHVT, hence, it is not critical to specify, whether stream 11 still contains some traces moisture or not.

The hot stream leaving the RHVT is supplied to a desuperheater, where it rejects heat to the ambient, operating in parallel to the conventional gas cooler (2–3). The cooled gas at point 13 is then joined with the evaporator exit 7, closing the cycle and providing inlet gas (1) to the compressor.

To set the superstructure into the the Maurer refrigeration cycle mode, flow through the throttle valve is set as zero, and the thermodynamic state is set equal for another set of system points:

$$\dot{m}_i = \dot{m}, \quad i \in \{1, 2, 3, 8\} \quad \text{and} \quad \dot{m}_{12} = \dot{m}_4 \tag{4}$$

$$\dot{m}_j = 0 \quad j \in \{5, 6\} \tag{5}$$

$$\Phi_8 = \Phi_3, \quad \Phi_{12} = \Phi_4 \tag{6}$$

To find mass flow rate and parameters in all system points, some additional equations are needed, as specified in the following subsection.

Hybrid mode, with some fraction of the flow directed to the TV, and another fraction supplied to RHVT can be of interest e.g. for off-design regulation. However, it is not modelled in the present paper as the results are expected to be between both 'plain' mode solutions.

2.1.2. Characteristic mass fractions. Mass and energy balances. Performance

For the Maurer model, a 3-fluid vortex tube is used, and its operation is characterized by two mass fractions:

Liquid Mass Fraction, relating the condensed liquid flow to the inlet stream:

$$\mathrm{LMF} = \frac{\dot{m}_{10}}{\dot{m}_8}, \tag{7}$$

Cold Mass Fraction, which needs an adapted definition. For standard vortex tubes, the cold mass fraction is commonly defined as the ratio of the cold outlet stream to the inlet stream. However, in the studied 3-fluid VT configuration it is meaningful to relate the cold, gaseous outlet stream to the overall mass flow rate of the *gaseous phase*:

$$\mathrm{CMF} = \frac{\dot{m}_{11}}{\dot{m}_8 - \dot{m}_{10}}, \tag{8}$$

Accordinlgy, the CMF describes how much of the gaseous phase, once the liquid is separated, is directed towards the cold exit.

To solve the set of mass and energy balance of the studied refrigeration system, the following equations are required:

Calorific functions for all system points

$$h_i = h(p_i, T_i) \ : \quad \text{enthalpy of the working medium} \tag{9}$$

$$s_i = s(p_i, T_i) \ : \quad \text{entropy of the working medium} \tag{10}$$

$$\dot{H}_i = \dot{m}_i h_i \ : \text{enthalpy flux} \tag{11}$$

Compression process with isentropic reference point 's'

$$s_{2s} = s_1 \quad \text{and} \quad h_{2s} = h(s_{2s}, p_2) \ : \quad \text{reference point identification} \tag{12}$$

$$\eta_C = \frac{h_{2s} - h_1}{h_2 - h_1} \ : \quad \text{compression isentropic efficiency} \tag{13}$$

Isenthalpic throttling (TV mode)

$$h_6 = h_5 \tag{14}$$

Vortex tube

$$\dot{m}_8 = \dot{m}_{10} + \dot{m}_{11} + \dot{m}_{13} \tag{15}$$

$$\dot{H}_8 = \dot{H}_{10} + \dot{H}_{11} + \dot{H}_{13} \tag{16}$$

Cold outlet junction

$$\dot{m}_{10} + \dot{m}_{11} = \dot{m}_{12} \tag{17}$$

$$\dot{H}_{10} + \dot{H}_{11} = \dot{H}_{12} \tag{18}$$

Hot outlet junction

$$\dot{m}_{13} + \dot{m}_7 = \dot{m}_1 \tag{19}$$

$$\dot{H}_{13} + \dot{H}_7 = \dot{H}_1 \tag{20}$$

The **coefficient of performance** has been defined as:

$$\mathrm{COP} = \frac{\dot{H}_7 - \dot{H}_4}{\dot{H}_2 - \dot{H}_1}, \tag{21}$$

which is valid both for the reference configuration and for the Maurer cycle.

2.1.3. Assumptions, thermodynamic analysis

For the Maurer model, the following assumptions have been done, partially based on a previous analysis [19]:

evaporator pressure: $p_1 = 3.5$ MPa;
evaporator outlet temperature: $T_1 = 0.16$°C (saturation);
compressor efficiency: $\eta_C = 0.85$;
minimum temperature difference for heat exchanger: $\Delta T_{\min} = 10$ K.
ambient temperature: $T_{amb} = 10 \ldots 40$°C.

Modelling has been performed for a unitary flow of $\dot{m}_1 = 1$ g/s, assuming that the thermodynamic quality of the system does not depend on system size.
A thermodynamic diagram of the reference refrigeration cycle is presented in Fig. 4(a), showing the reference specific cooling capacity between states 6 and 7.
The 3-fluid vortex tube is represented in Fig. 4(b). As can be concluded, the hot outlet (H) can only be produced if there is an intrinsic energy transfer from the cold gaseous stream to the hot one, since the specific enthalpy of H is higher than the inlet enthalpy 8.
Fig. 5(a) shows the junction of both cold RHVT outlets: the liquid and the gaseous one, and it shows the position of the junction point 12 between both saturation states 10 and 11, with exact position depending on the proportion of the mixed fluxes. It can also be seen that the cooling capacity of the RHVT-based system can be higher than the reference capacity provided that point 12 is situated left from the reference point 6. Accordingly, only a certain set of solutions can provide a positive performance effect.
The operation of the desuperheater is shown in Fig. 5(b). It can be seen that heat can be rejected to the ambient air in parallel with the gas cooler, and depending on the ambient temperature and the heat exchange performance, a temperature T_{13} is obtained. To close the cycle, flux 13 is mixed with flux 7 leaving the evaporator and then the joined flux is directed to the cycle compressor.

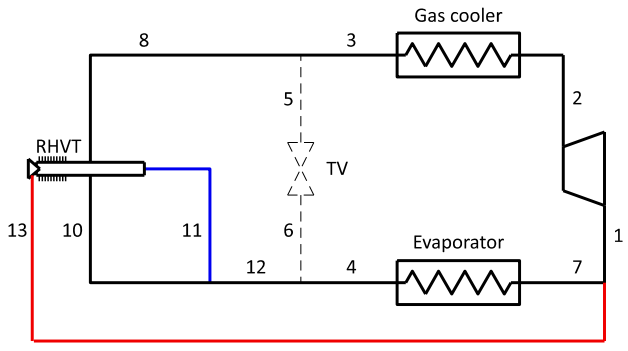

Figure 3: An alternative structure of the Maurer model with the desuperheater integrated into the vortex tube

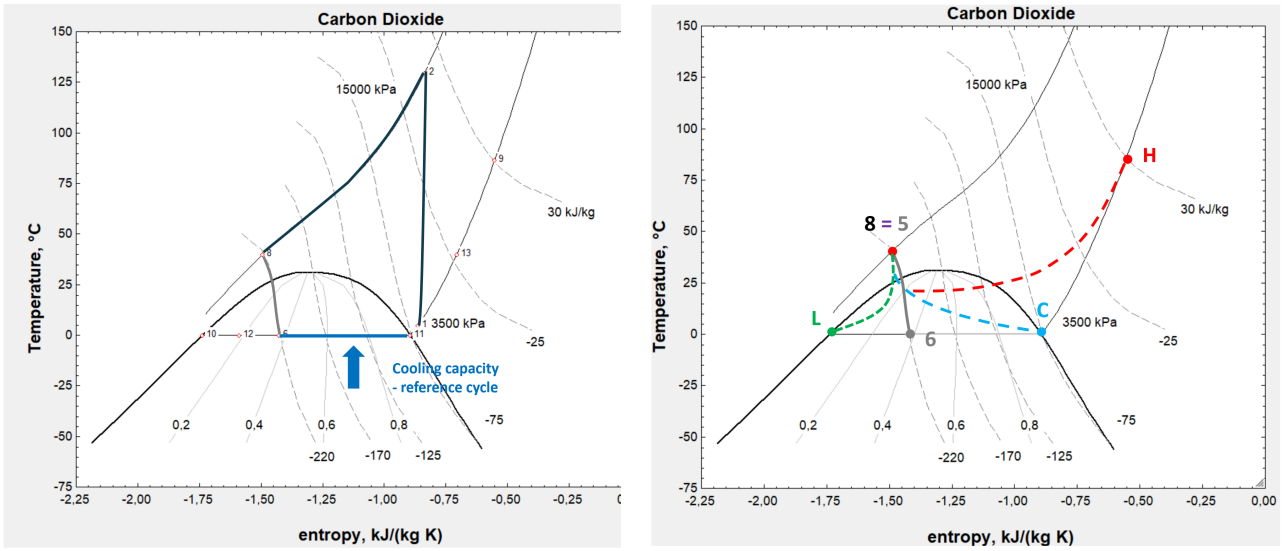

Figure 4: a) Temperature-entropy diagram of the reference refrigeration cycle, and the reference cooling capacity, (b) Temperature-entropy diagram of the 3-fluid vortex tube flow compared to the throttling process

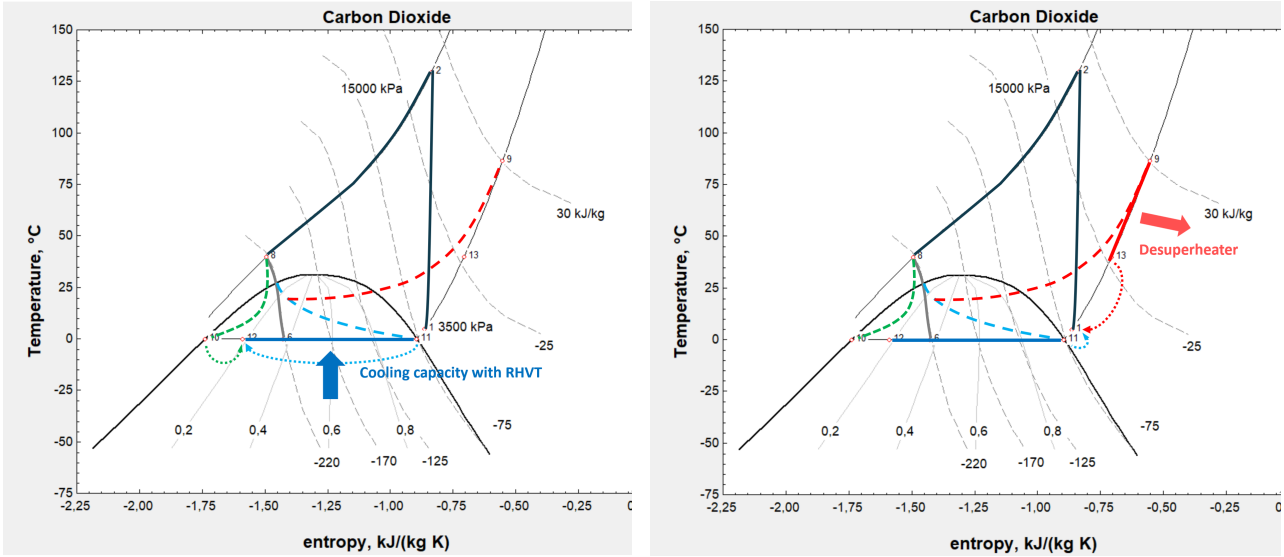

Figure 5: Temperature-entropy diagram of the Maurer cycle with RHVT: (a) the increased cooling capacity, (b) the use of desuperheater and the closure of the cycle

In addition to the energy analysis of the process, an **exergy test** has been applied to verify whether the obtained set of solution is in agreement with the 2nd law of thermodynamics. For each point of the system, a specific exergy has been calculated as:

$$b = h - h_0 - T_0(s - s_0) \tag{22}$$

where the reference temperature T_0 is substituted in kelvins. The total exergy flux for any system point i equals:

$$\dot{B}_i = \dot{m}_i b_i \tag{23}$$

The exergy test checks whether the irreversibility $\dot{I}_{VT}$ of the vortex tube is positive:

$$\dot{I}_{VT} = \dot{B}_8 - \dot{B}_{10} - \dot{B}_{11} - \dot{B}_{12} \tag{24}$$

If $\dot{I}_{VT} > 0$, then the system fulfills the 2nd law of thermodynamics at the calculated boundary points. For $\dot{I}_{VT} > 0$ it can be concluded that the solution does meet the energy balance, yet it is impossible to obtain in light of the 2nd law of thermodynamics, and the obtained theoretic result has to be rejected.

2.2. The Keller model

2.2.1. Model structure

The structure of the **Keller Model** is presented in Fig 6.

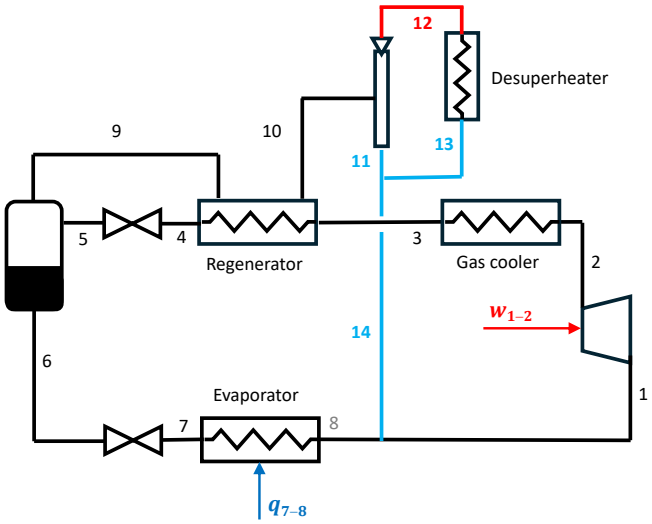

Figure 6: A structure of the Keller model

The cycle contains a compressor (Process 1–2), a gas cooler (2–3) and an evaporator (7–8), which do not differ with respect to the reference refrigeration cycle. However, the throttling process is divided into 2 stages with an intermediate pressure. The first throttle valve (4–5) discharges the fluid into a separator, where the liquid phase is collected and directed to the 2^{nd} stage of throttling. The gaseous phase (point 9) is returned 'upstream' of the cycle to a heat exchanger (regenerator), where it is heated by the main fluid (point 3) leaving the gas cooler. Then, the superheated gasoeus phase (10) is directed to a vortex tube producing a hot fluid (12) and a cold fluid (11). The hot fluid is then cooled in a desuperheater (12–13) and then joint with the cold fluid. The joined cold agent (14) is returned to the main cycle at the compressor inlet, providing a reduction of compression work.

Since the Keller model operates with two throttle valves and an intermediate pressure, the reference standard refrigeration cycle is not included in the structure to avoid any graphical or logical mismatch. Instead, the standard refrigeration cycle inscribed into the Maurer model superstructure is used as a reference.

2.2.2. Characteristic mass fractions. Mass and energy balances. Performance

For the Keller model, the set of equations describing the operation of the compressor and the 1st step gas cooler is the same as for the Maurer model. The remaining elements of the system are described with the following set of equations:

Regenerator

$$\dot{H}_3 - \dot{H}_4 = \dot{H}_{10} - \dot{H}_9 \tag{25}$$

$$T_{10} = T_3 - \Delta T_{\min} \tag{26}$$

throttle valve 1

$$h_5 = h_4 \tag{27}$$

Seperator tank

$$\dot{H}_5 = \dot{H}_6 + \dot{H}_9 \tag{28}$$

$$\dot{m}_9 = x_5 \dot{m}_5 \tag{29}$$

$$\dot{m}_6 = (1 - x_5)\dot{m}_5 \tag{30}$$

throttle valve 2

$$h_7 = h_6 \tag{31}$$

Evaporator

$$x_8 = 1 \tag{32}$$

Vortex tube

$$\dot{m}_{10} = \dot{m}_{11} + \dot{m}_{12} \tag{33}$$

$$\dot{H}_{10} = \dot{H}_{11} + \dot{H}_{12} \tag{34}$$

Desuperheater

$$T_{12} = T_{amb} + \Delta T_{\min} \tag{35}$$

Cold outlet junction

$$\dot{m}_{12} + \dot{m}_{13} = \dot{m}_{14} \tag{36}$$

$$\dot{H}_{12} + \dot{H}_{13} = \dot{H}_{14} \tag{37}$$

Compressor inlet junction

$$\dot{m}_8 + \dot{m}_{14} = \dot{m}_1 \tag{38}$$

$$\dot{H}_8 + \dot{H}_{14} = \dot{H}_1 \tag{39}$$

For the regenerator, it should be noted that $\dot{m}_3 > \dot{m}_9$ and the pinch point occurs at the hot side of the counter-current heat exchanger.
The **coefficient of performance** has been defined as:

$$\mathrm{COP} = \frac{\dot{H}_8 - \dot{H}_7}{\dot{H}_2 - \dot{H}_1}, \tag{40}$$

which is valid for Keller cycle. For the reference standard refrigeration cycle, Eq. (21) should be used.

2.2.3. Assumptions, thermodynamic analysis

For the Keller model, the model uses the same assumptions as for the Maurer cycle, with two additional assumptions:

intermediate pressure: $p_5 = 5700$ kPa [20];
hot-end temperature difference: $\Delta T_{hot} = T_{11} - T_{10} = 20$ K

Contrary to the 3-fluid VT with fixed liquid mass fraction, the energy balance is not sufficient to predict the outlet temperature, since many possible solutions fulfill the energy balace. Accordingly, the hot-end temperature difference was assumed as a parametric input value.
Modelling has been performed for a unitary flow of $\dot{m}_1 = 1$ kg/s, assuming that the thermodynamic quality of the system does not depend on system size.
A thermodynamic diagramm of the **Keller Model** is presented in Fig 7. As it can be seen the

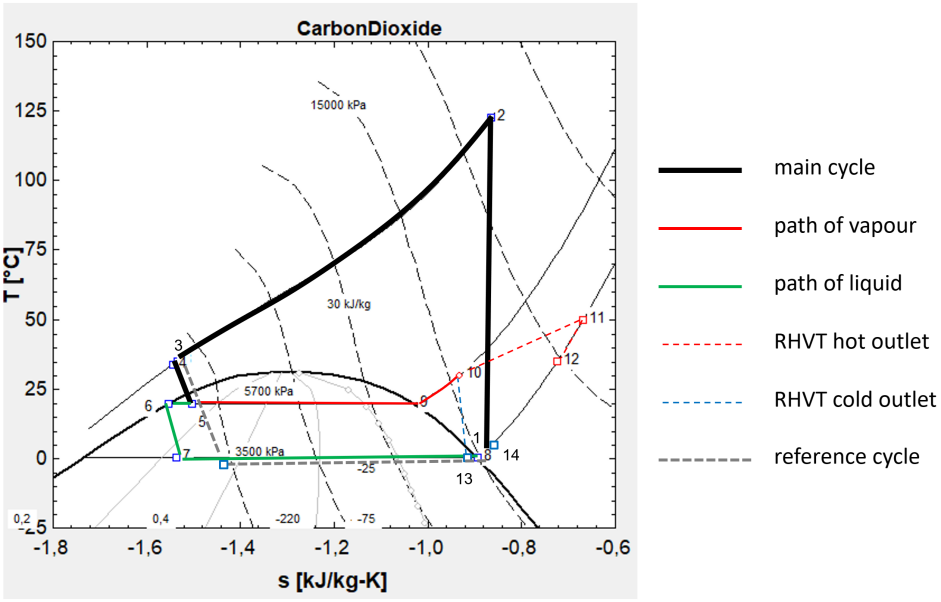

Figure 7: A thermodynamic diagram of the Keller model

the $T - s$ diagram, the path of the main cycle comprising compression (1–2) and cooling (2–3) correponds to the reference cycle. Due to the heat exchange with a colder fluid, the temperature is slightly reduced to (4), and then the first stage of throttling (4–5) is carried out for the main fluid. At point (5), the fluid enters the separator, where it is split to a liquid (6) and a saturated gas (9). The liquid phase is throttled (6–7) and directed to the evaporator (7–8), point (8) is at saturation. The gaseous phase from the separator (9) is set into a heat exchange with the main fluid (3), and due to small quantity of the gas phase, it can be noticeably heated to point (10). From that point, the superheated gas is directed to the vortex tube, where it is split in two exit streams: the hot (11) and the cold one (13). The hot fluid (11) can be cooled in a desuperheater to state (12), and then the fluxes (12) and (13) are collected to point (14), slightly superheated above the saturation line.
The possible improvement of COP results from a superposition of several, partially contradictory factors:

+ the 'regeneration of cold' allows the main stream to be cooled deeper than in the conventional gas cooler ($T_4 < T_3$); however, the difference is not large;
+ the enthalpy of liquid entering the evaporator at point (7) is significantly lower than in the reference case; the specific cooling capacity per 1 kg agent increases;
– however, the flux of fluid in the evaporator is lower than in the reference case, since a small share of gaseous fluid is collected in the evaporator;

– , the mixed fluid (14) returning from the vortex tube section is sightly above saturation, which can slightly increase the compression work.

As it can be concluded, only a selected range of parameters provides an overall positive effect.

2.3. The Vortex Tube numerical model

While the operation of a vortex tube as a thermal separation device has been studied by the project team and other researchers, and the process of mass separation of gasses of different density is under study within the ongoing ATHLETE project, there is little to no information on the RHVT operation for multiphase flows. For both studied configurations (Maurer and Keller) the occurrence of the liquid phase should be considered, provided that VT outlet parameters are below the critical point of CO2. While the Maurer configuration explicitly requires the liquid to be condensed, the Keller configuration is expected to work with the gas phase only. However, as shown in the Results section, a small share of liquid is difficult to avoid at the cold outlet, which should be considered in a more detailed modelling and design.

In order to have a first insight, a 2D layout implemented in Ansys Fluent has been realised to understand the possibility to liquefy and then separate the liquid droplets of CO_2. Vortex tube proportions and dimensions have been carefully scaled according to the ones presented in [21]. For this preliminary study, a steady state simulation has been considered, in fact, the idea behind the simulation campaign was to establish the effective capability of the solver to capture phase change while the CO_2 flow was expanding within the RHVT. Thus, a Volume of Fluid (VOF) multiphase model has been considered, while the two CO_2 phases have been implemented like independent fluids with real gas properties as per NIST tables already implemented into the considered solver.

The computational domain is reported in the next Fig. 8, characterized by an inlet with imposed swirling condition to make the system capable of separating hot and cold streams. The hot outlet is represented by the small annulus located rightward, while the cold outlet is the larger section located at the left side of the domain. The inlet mass flow inlet has been evenly distributed

Figure 8: Schematc representation of the evaluated RHVT.

across the four inlet ducts with CO_2 at 13 MPa and 47 °C, while the two outlet sections are pressure outlet ones with imposed pressure of about 3.5 MPa.

3. Results and discussion

3.1. The Maurer model

As a result of model calculations, three values are of particular significance:

1. the hot-outlet vortex tube temperature T_9;
2. the calculated system COP;
3. increment of the COP compared to the reference value $\mathrm{COP}_{\mathrm{ref}}$

Moreover, a reference liquid mass fraction was determined as:

$$\mathrm{LMF}_{\mathrm{ref}} = 1 - x_6 \tag{41}$$

where x_6 represents the quality (mass fraction of vapour) obtained in the reference refrigeration cycle with a throttle valve.

Values of the hot-outlet vortex tube temperature T_9 in terms of the CMF and LMF parameters are shown in Table 1.

Table 1: Calulated hot-outlet RHVT temperature for the Maurer model. Ambient temperature $T_{amb} = 30°$C.

CMF	**LMF**						
	0.5	0.6	0.6307	0.7	0.8	0.9	1
0	0.17	0.17	0.17	38.4	171.2	(552.0)	–
0.1	0.17	0.17	0.17	43.4	191.9	(609.5)	–
0.3	0.17	0.17	0.17	58.3	250.3	(769.4)	–
0.5	0.17	0.17	0.17	86.5	352.3	(R)	–
0.7	0.17	0.17	0.17	154.3	576.8	(R)	–
0.9	R	0.17	0.17	476.9	R	(R)	–

Grey colour indicates unfavourable saturation temperature or a physically unlikely value
R denotes hot-outlet temperature out of admissible range.
The (–) sign denotes lack of numerical convergence.
Values in brackets are rejected due to the 2nd law violation.

The Table presents selected results for LMF ranging from 0.5 to 1 with the reference value $\mathrm{LMF_{ref}}$ explicitly included. This value is different for various ambient temperatures. It can be seen, that for LMF $\leqslant \mathrm{LMF_{ref}}$, the vortex tube is not able to produce a superheated vapour stream, and all 3 fluids leaving the device are at saturation temperature. Accordingly, no additional cooling effect can be produced, since the desuperheater fails to reject any extra heat, while the flux of agent directed to the evaporator is lower than in the reference case.

In the studied example, LMF$= 0.7$ provides a set of interesting results, with hot-end temperatures ranging from 38 to 86°C and more. However, results above 100°C have been classified as *unlikely*, since the current knowledge on vortex tube operation fails to confirm this range of thermal stratification.

Furthermore, some values, which are unlikely to appear anyway, are presented in brackets as they have to be rejected due the 2nd law violation identified by the exergy test described in the Methodology section.

Table 2 shows the calculated increment of COP for the Maurer configuration, with respect to the reference $\mathrm{COP_{ref}}$ which is indicated for each studied ambient temperature. While Table 1 shows the caclulated hot-end temperatures for one selected ambient temperature $T_{amb} = 30°$C, the COP Table 2 shows more results as a function of the ambient temperature ranging from 10 to 40°C. As it can be seen, results may be classified into several categories:

1. negative results: The COP has deteriorated compared to the reference refrigeration system with a throttle valve;
2. positive and potentially viable results, corresponding to hot-end temperatures up to 100°C;
3. positive yet unlikely results, corresponding to hot-end temperature exceeding 100°C; for example, for the ambient temperature of 30°C, the maximum obtainable COP increment is 5.0%, while all higher values would require higher hot-end temperatures from the vortex tube. While thermodynamically correct, these values are not supposed to be obtainable in real conditions;
4. positive yet invalid results, with negative exergy test value: $I_{TV} < 0$. The value of I_{TV} is not displayed in the table yet it was controlled in the modelling process;
5. values out of range (R): the model converged with a warning that CO_2 temperature is out of range; these results are mostly also invalid from the exergy perspective and they are not displayed numerically;

6. lack of convergence (–): the model failed to provide any numerical results.

3.2. The Keller model

For the Keller model, results depend on three main parameters: (1) the ambient temperature T_{amb}, (2) the cold mass fraction CMF and (3) the hot-end temperature difference ΔT_H, describing the vortex tube quality. Results of the COP increment are shown in Table 3.

It can be seen, that contrary to the Maurer Model, lower ambient temperatures do not allow the system to work (i.e. the thermodynamic model failed to converge). Only a limited set of results was possible to obtain for higher ambient temperatures of 30 and 40°C. Interestingly, all values of COP increment are positive, except for the case of CMF = 1 at 30°C ambient temperature.

In this particular case, the Keller model becomes equivalent with a throttle valve, since the hot outlet of the VT remains closed. However, the same cofiguration does provide a minimum COP increment for higher ambient temperature. This is supposed to occur due to the existence of the regenerator, where part of the cold agent helps to cool the main fraction of gas leaving the compressor. However, the imposed minimum temperature differences cancel this effect for lower ambient temperatures.

Table 4 shows the cold-end temperature of gas leaving the vortex tube. It can be seen that it corresponds to the saturation temperature for certain points of the analysis, while being slightly superheated for higher cold mass fractions. Accordingly, one can observe that the vortex tube is working close to the saturation conditions at the outlet.

3.3. The Vortex Tube numerical model

In this section, numerical results obtained thanks to the model previously presented in Fig. 8 are shortly reported. For this preliminary analysis only a single operating point has been taken under consideration. The following figures show the capabilities of the component to locally liquefy the fluid, entering the system in vapor conditions, and the Mach number distribution.

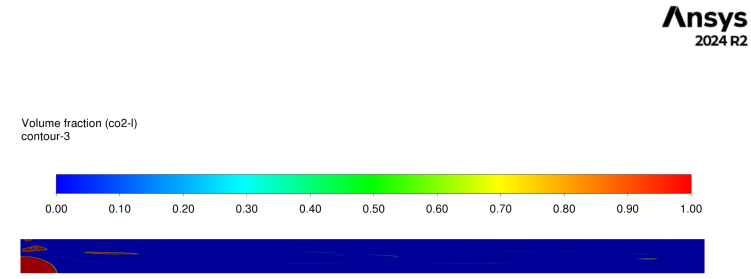

CO_2 liquid fraction distribution along the Vortex Tube.

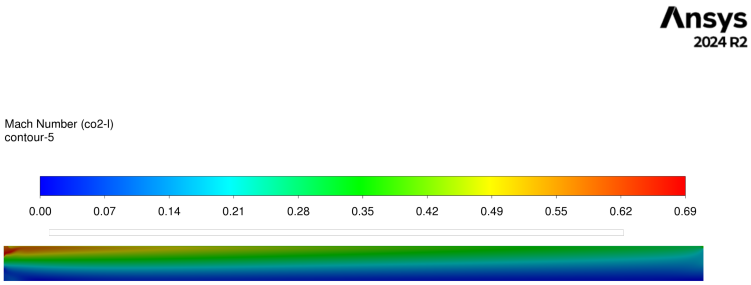

Mach number distribution along the Vortex Tube.

Figure 9: CO_2 liquid and Mach number distribution along the RHVT operating at steady state.

Figure 9 clearly demonstrates the system's capability to effectively liquefy the incoming gas. Notably, the core region of the flow is predominantly characterized by the vapour phase (dark blue), whereas the areas in the proximity of cold outlet is characterized by liquefied CO_2, thus,

Table 2: The calculated increment of COP for the Maurer configuration

A. $T_{amb} = 10°C$, $LMF_{ref} = 0.8418$, $COP_{ref} = 2.665$,							
CMF	**LMF**						
	0.5	0.6	0.7	0.8	0.8418	0.9	1
0	−46.2%	−34.2%	−21.7%	−8.8%	−3.2%	4.7%	–
0.1	−45.7%	−33.7%	−21.3%	−8.4%	−2.9%	5.0%	–
0.3	−44.7%	−32.6%	−20.3%	−7.7%	−2.3%	5.4%	–
0.5	−43.5%	−31.6%	−19.4%	−6.9%	−1.6%	5.8%	–
0.7	R	R	R	−6.2%	−1.0%	6.2%	–
0.9	–	–	R	−5.4%	−0.3%	–	–
1.0	–	–	–	–	–	–	–
B. $T_{amb} = 20°C$, $LMF_{ref} = 0.7409$, $COP_{ref} = 2.345$,							
CMF	**LMF**						
	0.5	0.6	0.7	0.7409	0.8	0.9	1
0	−41.2%	−27.5%	−13.2%	−7.1%	2.0%	18.0%	–
0.1	−40.4%	−26.8%	−12.5%	−6.4%	2.5%	18.3%	–
0.3	−38.8%	−25.2%	−11.0%	−5.1%	3.7%	19.0%	–
0.5	−37.1%	−23.5%	−9.5%	−3.7%	4.9%	(19.7%)	–
0.7	–	−21.8%	−8.0%	−2.2%	6.1%	R	–
0.9	–	–	−6.4%	−0.7%	7.4%	–	–
1	–	–	–	–	–	–	–
C. $T_{amb} = 30°C$, $LMF_{ref} = 0.6307$, $COP_{ref} = 1.997$,							
CMF	**LMF**						
	0.5	0.6	0.6307	0.7	0.8	0.9	1
0	−33.3%	−17.4%	−12.3%	−0.4%	17.9%	(37.5%)	–
0.1	−32.2%	−16.3%	−12.7%	0.7%	18.7%	(38.0%)	–
0.3	−30.0%	−14.0%	−8.9%	2.8%	20.4%	(39.0%)	–
0.5	−27.6%	−11.6%	−6.6%	5.0%	22.2%	–	–
0.7	−25.0%	−9.0%	−4.1%	7.3%	24.0%	–	–
0.9	–	−6.3%	−1.4%	9.7%	–	–	–
1.0	–	–	–	–	–	–	–
D. $T_{amb} = 40°C$, $LMF_{ref} = 0.5059$, $COP_{ref} = 1.605$,							
CMF	**LMF**						
	0.5	0.5059	0.6	0.7	0.8	0.9	1
0	−19.6%	−18.5%	0.1%	21.4%	44.5%	(69.7%)	–
0.1	−18.1%	−17.0%	1.7%	22.9%	(45.8%)	R	–
0.3	−15.0%	−13.8%	4.9%	26.0%	(48.3%)	R	–
0.5	−11.5%	−10.2%	8.4%	29.2%	(50.9%)	R	–
0.7	−7.7%	−6.4%	12.2%	32.6%	R	R	–
0.9	−3.6%	−2.2%	16.2%	–	–	–	–
1.0	–	–	–	–	–	–	–

Grey values indicate negative ΔCOP.
R denotes hot-outlet temperature out of admissible range.
The (–) sign denotes lack of numerical convergence.
Values in brackets are rejected due to the 2nd law violation.

Table 3: Calculated increment of COP for the Keller configuration

A. $T_{amb} = 30°C$, $COP_{ref} = 1.997$			
CMF	ΔT_{hot}		
	20	30	40
0	–	–	–
0.1	–	–	–
0.3	–	–	–
0.5	0.7%	–	–
0.7	0.4%	0.8%	–
0.9	0.1%	0.3%	0.4%
1.0	0.0%	0.0%	0.0%
B. $T_{amb} = 40°C$, $COP_{ref} = 1.605$			
CMF	ΔT_{hot}		
	20	30	40
0	–	–	–
0.1	R	R	–
0.3	2.7%	4.3%	5.9%
0.5	2.3%	3.4%	4.5%
0.7	1.9%	2.5%	3.2%
0.9	1.4%	1.6%	1.9%
1.0	1.2%	1.2%	1.2%

R denotes hot-outlet temperature out of admissible range.
The (–) sign denotes lack of numerical convergence.

lower-temperature regions primarily contain the liquid phase (red). Moreover, one can observe how the majority of the liquid fraction is located near the outlet region, whereas lower static temperature have been reached, allowing the condensation process of the incoming flow-rate, some secondary structures are generated, but they are vapourized again being in contact with the inner hooter flow. It is worth highlighting how the inlet boundary conditions have been imposed assuming 100% of vapour fraction. Thus, the condensation process occurs being locally reached the condensation temperature at the target pressure of 3.5 MPa. Results obtained based on the proposed configuration are presented in Table 5.

4. Conclusions

The performed modelling approached two alternative cofigurations for a CO_2-based refrigeration cycle with an integrated vortex tube: the Maurer model, including a concept of a 3-fluid vortex tube with an additional liquid outlet, and the Keller model, based on a conventional two-outlet vortex tube.

The modelling approach combined basic mass and energy balance equations including real-fluid properties of CO_2, and additional verification measures: (1) the exergy test, aiming to verify the thermodynamic possiblity of the obtained solution from the 2nd law point of view, and (2) a preliminary numerical model, aiming to verify if it is possible to handle the liquid phase within the vortex tube.

It has been demonstrated that only a selected, narrow set of steering parameters, such as the cold mass fraction, hot-end temperature and (for the Maurer model) the liquid mass fraction is able to yield a positive COP increment. Other ranges of parameters either fail to provide any thermodynamic improvement, or they seem to be invalid theoretic values not possible to be confirmed by experiments. Still, in the studied narrow range of parameters the predicted COP increment is noticeable , reaching 5% for the Maurer model, and 5.9% for the Keller model. This suggest a potential for further parametric optimisation and technology development.

Table 4: Cold-outlet temperature of the vortex tube in the Keller model

A. $T_{amb} = 30°\mathrm{C}$			
CMF	ΔT_{hot}		
	20	30	40
0.3	–	–	–
0.5	0.17	–	–
0.7	0.17	0.17	–
0.9	0.33	0.17	0.17
1.0	4.09	4.09	4.09
B. $T_{amb} = 40°\mathrm{C}$			
CMF	ΔT_{hot}		
	20	30	40
0.3	0.17	0.17	0.17
0.5	0.17	0.17	0.17
0.7	2.146	0.17	0.17
0.9	12.59	11.75	10.94
1.0	16.69	16.69	16.69

The (–) sign denotes lack of numerical convergence.

Table 5: Steady-state results for the 2D simulation.

Section	$\dot{m}$, $\mathrm{kg/s}$	T, $°\mathrm{C}$	T_t, $°\mathrm{C}$
Inlet	0.0880	35	47
Cold outlet	0.0260	6	7
Hot outlet	0.0620	55	60

The obtained results, despite their preliminary character, clearly indicate a low technology readiness level (TLR 0–1). Refrigeration cycles with a vortex tube remain a promising yet challenging thermodynamic concept requiring further fundamental research, primarily focused on the 2-phase operation of the working fluid.

Acknowledgments

This research has been supported by the National Science Centre of Poland within the 'ATHLETE' project NCN-Opus No. 2021/43/B/ST8/03320 (UMO-2021/43/B/ST8/03320).

Nomenclature

Latin symbols

- b specific exergy, $\mathrm{kJ/kg}$
- $\dot{B}$ exergy flux, $\mathrm{kJ/s}$
- h specific enthalpy, $\mathrm{kJ/kg}$
- $\dot{H}$ enthalpy flux, $\mathrm{kJ/s}$
- $\dot{I}$ irreversibility rate, $\mathrm{kJ/s}$
- $\dot{m}$ mass flow rate, $\mathrm{kg/s}$
- p pressure, kPa
- T temperature, $°\mathrm{C}$
- T_0 reference temperature for exergy, K ($T_0 = 281$ K)
- v specific volume, $\mathrm{m^3/kg}$
- x vapour quality

Greek symbols

η	efficiency
Φ	thermodynamic state vector $\Phi = (p, T, v)$

Subscripts and superscripts

amb	ambient
C	compressor
ref	reference
t	total
VT	vortex tube

Acronyms

CMF	Cold mass fraction
COP	Coefficient of performance
LMF	Liquid mass fraction
RHVT	Ranque-Hilsch vortex tube

References

[1] G. Ranque *et al.*, "Experiments on expansion in a vortex with simultaneous exhaust of hot air and cold air," *J. Phys. Radium*, vol. 4, no. 7, pp. 112–114, 1933.

[2] R. Hilsch, "Die expansion von Gasen im Zentrifugalfeld als Kälteprozess," *Zeitschrift für Naturforschung A*, vol. 1, no. 4, pp. 208–214, 1946.

[3] T. J. Bruno, "Laboratory applications of the vortex tube," *Journal of chemical Education*, vol. 64, no. 11, p. 987, 1987.

[4] S. Yuksel and A. Onat, "Investigation of CNC turning parameters by using a vortex tube cooling system," *Acta Physica Polonica A*, vol. 127, 2015.

[5] A. N. Shmroukh, M. Attalla, A. A. E.-N. Abd El, *et al.*, "Experimental investigation of a novel sea water desalination system using Ranque-Hilsch vortex tube," *Applied Thermal Engineering*, vol. 149, pp. 658–664, 2019.

[6] J. Keller and M. Göbel, "Die thermodrossel: eine anlage zur entspannung komprimierter flüssigkeiten unter wärmeabgabe," *KI. Luft-und Kältetechnik*, vol. 33, no. 2, pp. 57–60, 1997.

[7] T. Maurer, "Patent de 197 48 083 a1," *Entspannungseinrichtung*, 1999.

[8] Y. Liu and J. Yu, "Review of vortex tube expansion in vapour compression refrigeration system," in *IOP Conference Series: Earth and Environmental Science*, vol. 153, p. 032021, IOP Publishing, 2018.

[9] D. Jing, G. Yan, Y. Li, T. Xiong, and G. Liu, "A review of refrigerant-based vortex tube separation characteristics: Devices, thermodynamic cycles and system experiments," *Energy*, vol. 320, p. 135334, 2025.

[10] F. Liang, J. Chen, and G. Tang, "Experimental investigation on the influence of drainage structure on vortex tube energy separation," *Applied Thermal Engineering*, vol. 271, p. 126363, 2025.

[11] D. Li, J. Baek, E. Groll, and P. Lawless, "Thermodynamic analysis of vortex tube and work output expansion devices for the transcritical carbon dioxide cycle," *4th IIR-Gustav Lorentzen Conference on Natural Working Fluids at Purdue*, pp. 463–470, 01 2000.

[12] Y. B. Xie, K. K. Cui, Z. C. Wang, and J. L. Liu, "Co2 trans-critical two stage compression refrigeration cycle with vortex tube," *Applied Mechanics and Materials*, vol. 52, pp. 255–

260, 2011.

[13] Y. F. Liu, C. J. Geng, and G. Y. Jin, "Vortex tube expansion transcritical co2 heat pump cycle," *Applied Mechanics and Materials*, vol. 190, pp. 1340–1344, 2012.

[14] R. Khera, A. Arora, and B. Arora, "Energy, exergy, environmental (3e) analyses and multi-objective optimization of vortex tube coupled with transcritical refrigeration cycle," *International Journal of Refrigeration*, vol. 167, pp. 137–151, 2024.

[15] Y. Li, G. Yan, Y. Yang, P. Dong, and G. Liu, "Thermodynamic analysis of new configurations of auto-cascade refrigeration cycles integrating the vortex tube," *Energy*, vol. 308, p. 132982, 2024.

[16] Z. Luo, W. Chen, X. Li, S. Lu, and F. Guo, "Performance improvement of transcritical co2 refrigeration cycle by integrating vortex tube expansion: Simulation and optimization," *Thermal Science and Engineering Progress*, vol. 45, p. 102078, 2023.

[17] K. Chen, F. Wang, N. Li, S. Liang, Y. Tian, Z. Li, and C. Guo, "Comprehensive experimental study of a transcritical co2 vortex tube," *Applied Thermal Engineering*, vol. 277, p. 127122, 2025.

[18] A. Mansour, R. Oberti, H. Nesreddine, D. Monney, and S. Poncet, "Performance of a transcritical co2 vortex tube: A first experimental campaign," *Thermal Science and Engineering Progress*, vol. 57, p. 103128, 2025.

[19] B. M. Mendecka, D. Chiappini, and G. Bella, "Cooling performance of an modified r744 air conditioning system with vortex tube and internal heat exchanger for an electric vehicle," tech. rep., SAE Technical Paper, 2021.

[20] J. Sarkar, "Cycle parameter optimization of vortex tube expansion transcritical co2 system," *International Journal of Thermal Sciences*, vol. 48, no. 9, pp. 1823–1828, 2009.

[21] H. Skye, G. Nellis, and S. Klein, "Comparison of cfd analysis to empirical data in a commercial vortex tube," *International Journal of Refrigeration*, vol. 29, no. 1, pp. 71–80, 2006.